Scattering rates for holes near the valence-band edge in semiconductors

T. BrudevollT. A. FjeldlyJ. Baek and M. S. Shur

Citation: Journal of Applied Physics **67**, 7373 (1990); doi: 10.1063/1.344524
View online: http://dx.doi.org/10.1063/1.344524
View Table of Contents: http://aip.scitation.org/toc/jap/67/12
Published by the American Institute of Physics

Scattering rates for holes near the valence-band edge in semiconductors

T. Brudevoll
Department of Electrical Engineering and Computer Science, Norwegian Institute of Technology, University of Trondheim, N-7034, Trondheim, Norway

T. A. Fjeldly
Department of Electrical Engineering and Computer Science, Norwegian Institute of Technology, University of Trondheim, N-7034, Trondheim, Norway, and Minnesota Supercomputer Institute, University of Minnesota, Minneapolis, Minnesota 55415

J. Baek[a] and M. S. Shur[b]
Department of Electrical Engineering and Minnesota Supercomputer Institute, University of Minnesota, Minneapolis, Minnesota 55455

(Received 9 October 1989; accepted 6 March 1990)

In this paper, we discuss and compare the rates for dominant scattering mechanisms for holes in semiconductors, including ionized impurity scattering, polar and nonpolar optical-phonon scattering, and inelastic acoustic deformation potential scattering. The scattering rates for these mechanisms have been reviewed for the purpose of finding reliable expressions to be used in Monte Carlo simulation of hole transport in *p*-type III-V semiconductor devices. In the scarce literature on hole scattering rates, we have found several discrepancies. Here, we present corrected rates for ionized impurity scattering and for scattering by polar optical phonons. In addition, we have derived new expressions for the *inelastic* acoustic deformation potential scattering rates where we also have included a series expansion for the phonon occupation number, beyond the equipartition approximation.

I. INTRODUCTION

The transport properties of holes in semiconductors are of great interest from both physics and device points of view. The valence bands are qualitatively very similar for nearly all semiconductors of interest, including silicon, III-V and most II-VI compounds. They include light- and heavy-hole bands and a split-off band, as shown schematically in Fig. 1. This means that the results obtained for the hole transport can be applied to a great variety of different semiconductor materials and devices—from silicon *p*-channel field-effect transistors (FETs) that are used in complementary metal-oxide-semiconductor (CMOS) technology, to bipolar transistors, heterostructure bipolar transistors (HBTs), compound semiconductor *p*-channel FETs, and optoelectronic devices such as lasers, light emitting diodes, etc.

Many modern devices utilizing hole transport have very small dimensions, in the submicrometer range, in order to alleviate problems related to a relatively small hole mobility. A full understanding of the hole transport in such structures requires accurate Monte Carlo simulations. Such simulations will also provide a starting point for devices utilizing two- and one-dimensional hole gases as well as holes in semiconductor regions under stress, with split light- and heavy-hole bands at the Γ point.

The physics involved in the Monte Carlo calculations is reflected in scattering rates for different scattering mechanisms. In this paper, we calculate and compare rates for ionized impurity scattering, polar and nonpolar optical-phonon scattering, and acoustic deformation potential scattering of holes. While the expression for nonpolar optical-phonon scattering is correctly described in the literature,[1] we have found that the previously published expressions for interband ionized impurity scattering,[1] interband polar optical-phonon scattering,[2–4] and the acoustic-phonon scattering rates[3–4] have to be corrected.

All numerical calculations in this paper are done for GaAs even though the analytical results apply to holes in all cubic semiconductors with exception of gapless semiconductors such as grey tin. Thus the derived expressions can be used for the Monte Carlo simulation of hole transport in all such semiconductor materials and in devices made from them. All the present scattering rates have been derived assuming parabolic bands, and the band warping is accounted for by the use of approximate overlap functions.

In Sec. II, we present corrected results for ionized impurity scattering. Rates for nonpolar optical-phonon scattering and the corrected polar optical-phonon scattering rates are presented in Sec. III. In Sec. IV, new results are derived for inelastic inter- and intravalley deformation potential scattering by acoustic phonons. Since the validity of the equipartition approximation for the phonon occupation number

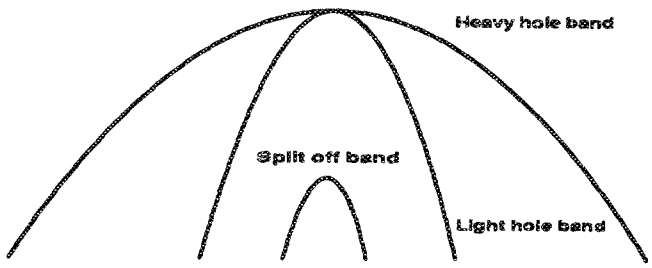

FIG. 1. Valence-band structure in common semiconductors.

[a] Present address: AT&T Bell Laboratories, Reading, PA 19612.
[b] Present address: Department of Electrical Engineering, University of Virginia, Charlottesville, VA 22901.

 0021-8979/90/127373-10$03.00

$N_{ph}(q)$ has been questioned,[3–7] we have adopted here a more general representation for $N_{ph}(q)$ according to Canali *et al.*[5] It turns out that the final expressions for the acoustic scattering rates are much more complicated for holes than for electrons. The results are discussed in Sec. V. Section VI contains a summary and concluding remarks.

II. IONIZED IMPURITY SCATTERING

The ionized impurity scattering rate for holes can be readily obtained by considering impurity centers with a screened Coulomb potential.[1] Here we present corrected results in terms of the following compact expression:

$$P_{if}^{im} = \frac{3e^4 N_i m_f F}{32\pi\hbar^3 \epsilon_0^2 \epsilon_S^2 k_i^2 k_f}, \tag{1}$$

where e is the electron charge, N_i is the density of ionized scatterers, ϵ_0 is the vacuum dielectric constant, and ϵ_S is the static relative dielectric permittivity of the semiconductor. The magnitudes of the initial-state wave vector k_i and the final-state wave vector k_f are related through the condition of energy conservation, which for elastic scattering simply becomes $k_f^2 = Mk_i^2$, where $M = m_f/m_i$ is the ratio between the final- and initial-state effective hole masses. A distinction between intra- and interband scattering is made through the factor F in Eq. (1):

$$F^{intra} = \frac{\beta^2 + 2k^2}{k^2} \ln\left(\frac{\beta^2}{\beta^2 + 4k^2}\right) + \frac{4}{3}\frac{3\beta^4 + 12\beta^2 k^2 + 8k^4}{\beta^2(\beta^2 + 4k^2)}, \tag{2a}$$

$$F^{inter} = \frac{\beta^2 + k_i^2 + k_f^2}{k_i k_f} \ln\left(\frac{\beta^2 + (k_i + k_f)^2}{\beta^2 + (k_i - k_f)^2}\right) - 4, \tag{2b}$$

where $\beta = (N_i e^2/k_B T \epsilon_0 \epsilon_S)^{1/2}$ is the inverse screening length, k_B is the Boltzmann constant and T is the absolute temperature. Note that $k = k_i = k_f$ for intraband scattering.

The impurity scattering rates given here can also be presented in a form displaying the effect of the overlap functions (see Sec. IV A) in a more explicit and symmetric manner. This was done in Ref. 1, but with nontrivial errors in the expression given for the interband rate.

The ionized impurity scattering rates for holes in GaAs are shown for different temperatures and impurity densities in Fig. 2. The parameters used are listed in Table I.

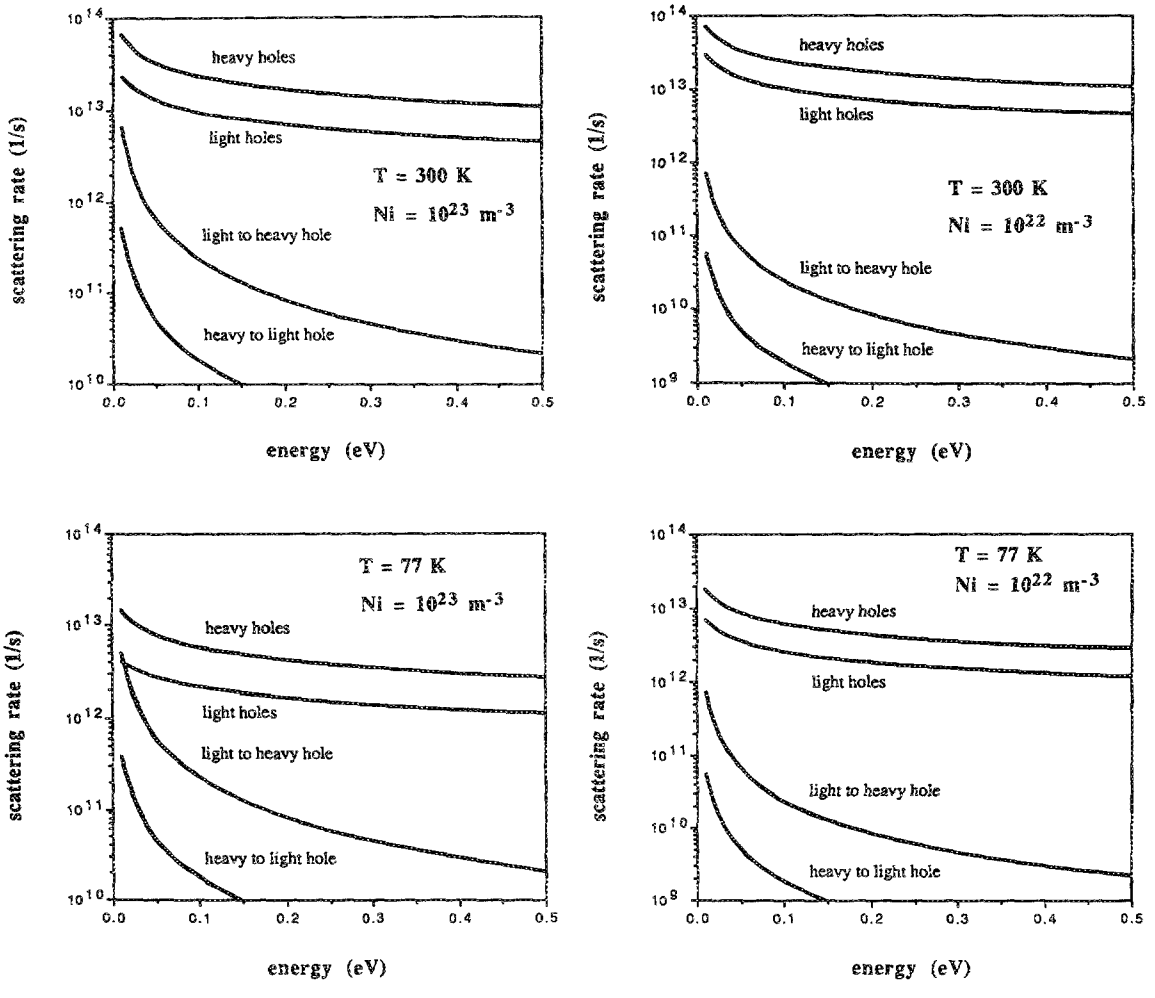

FIG. 2. Ionized impurity scattering rates for holes in GaAs for different temperatures and impurity densities.

TABLE I. List of parameters for GaAs.

$m_h = 0.45 m_0$ (heavy-hole mass, m_0: free-electron mass)[a]
$m_l = 0.082 m_0$ (light-hole mass)[a]
$\epsilon_S = 12.9$[a]
$\epsilon_\infty = 10.92$[a]
$\hbar\omega_0 = 0.035$ eV[a]
$\rho = 5360$ kg/m^3 [a]
Velocity of sound:
$s_l = 4730$ m/s[a]
$s_t = 3340$ m/s[a]
$s = (s_l^2/3 + 2s_t^2/3)^{1/2}$[b]
$s = 3860$ m/s
Elastic constants:
$C_{11} = 11.88\times10^{10}$ N/m^2 [b]
$C_{12} = 5.38\times10^{10}$ N/m^2 [b]
$C_{44} = 5.94\times10^{10}$ N/m^2[b]
$C_l = (3C_{11} + 2C_{12} + 4C_{44})/5$[b]
$C_t = (C_{11} - C_{12} + 3C_{44})/5$[b]
Deformation potential constants:
$a = 3.1$ eV[b]
$b = -1.7$ eV[b]
$d = -4.4$ eV[b]
$E_1 = (s/s_l)\Xi_{\rm eff} = (s/s_l)[a^2 + (C_l/C_t)(b^2 + d^2/2)]^{1/2}$[b,c]
$E_1 = 5.6$ eV
Optical-phonon coupling constant:
$(DK)^2 = 4(\omega_0/s_l)^2 E_1^2$[d,e,f]
$(DK)^2 = 1.58\times10^{22}$ eV^2/m^2

[a] M. Neuberger, *Handbook of Electronics Materials* (Plenum, New York, 1971), Vol. 2.
[b] J. D. Wiley, Solid State Commun. 8, 1865 (1970).
[c] The theoretical value $E_1 (\equiv E_{ac}) = 3.6$ eV given in footnote b is incorrect by a factor $\sqrt{2}$ owing to an error in Eq. (3) of that reference. When this error is corrected, the correspondence between theoretical and experimental values for E_1 is substantially improved.
[d] It should be emphasized that E_1 and $(DK)^2$ were determined experimentally at a time when the role of optical-phonon scattering in hole transport was still controversial; see footnote b. The factor 4 in the expression for $(DK)^2$ is based on experiments and hence is subject to uncertainty (footnote b).
[e] Reference 3.
[f] E. M. Conwell, *High Field Transport in Semiconductors* (Academic, New York, 1967).

III. OPTICAL-PHONON SCATTERING

A. Polar optical-phonon scattering

The scattering rate for holes by polar optical phonons was first calculated in Ref. 2. Unfortunately, the rates published for interband scattering have errors. These errors have propagated into Refs. 3 and 4, where also the rate for nonpolar optical scattering and for polar optical intraband scattering have become too large by a factor of 2. The correct result for inter- and intraband polar optical-phonon scattering can be expressed as

$$P_{if}^{\rm po} = \frac{e^2\omega_0 m_f}{4\pi\epsilon_0\hbar^2}\left(\frac{1}{\epsilon_\infty} - \frac{1}{\epsilon_S}\right)\begin{Bmatrix} N_0 \\ N_0+1 \end{Bmatrix}\frac{\Psi H}{k_i}, \tag{3}$$

where N_0 is the optical-phonon occupation number, and the factors N_0 and $N_0 + 1$ refer to absorption and emission of an optical phonon, respectively. Note that emission is only possible for initial hole energies larger than the optical-phonon energy $\hbar\omega_0$. For these inelastic processes, the condition of energy conservation now leads to the relationship $k_f^2 = M(k_i^2 \pm 2m_i\omega_0/\hbar)$ between the initial- and final-state wave vectors, where the upper and lower signs refer to absorption and emission, respectively. ϵ_∞ is the high-frequency relative dielectric permittivity of the semiconductor. Furthermore, $\Psi = \ln|(k_i + k_f)/(k_i - k_f)|$ and the H factors for intra- and interband scattering are

$$H^{\rm intra} = [1 + 3\Phi(\Phi - \Psi^{-1})]/4, \tag{4a}$$

$$H^{\rm inter} = 3[1 - \Phi(\Phi - \Psi^{-1})]/4, \tag{4b}$$

where $\Phi = (k_i^2 + k_f^2)/2k_ik_f$. The polar optical-phonon scattering rates in GaAs versus initial hole energy are shown in Fig. 3 for different temperatures. The parameters used are listed in Table I.

B. Nonpolar optical-phonon scattering

The following scattering rate for holes by the nonpolar optical-phonon mechanism was derived by Costato and Reggiani[1]:

$$P_{if}^{\rm npo} = \frac{(DK)^2 m_f^{3/2}}{2\sqrt{2}\pi\rho\hbar^3\omega_0}(E \pm \hbar\omega_0)^{1/2}\begin{Bmatrix} N_0 \\ N_0+1 \end{Bmatrix}, \tag{5}$$

where $(DK)^2$ is the optical-phonon coupling constant, ρ is the density of the semiconductor material, and E is the initial hole energy. The upper and lower sign in the square root correspond to absorption and emission of an optical phonon, respectively. Also, the factors N_0 and $N_0 + 1$ refer to absorption and emission of an optical phonon, respectively.

The nonpolar optical-phonon scattering rates in GaAs versus initial hole energy are shown in Fig. 4 for different temperatures. The parameters used are listed in Table I.

IV. INELASTIC ACOUSTIC DEFORMATION POTENTIAL SCATTERING

As discussed by Canali *et al.*,[5] special care must be taken in treating charge carrier scattering by acoustic phonons in Monte Carlo calculations. Although the energy exchange between charge carriers and the lattice is small for a single scattering event, this exchange is necessary for obtaining correct stationary conditions at low electric fields and low temperatures. By treating the acoustic phonon scattering as elastic processes, an artificial warming of the carrier gas will take place in the electric field until the temperature of the carrier gas has risen sufficiently to induce other inelastic processes. In order to obtain the correct carrier energy balance, it is also necessary to calculate the energy exchange in each scattering event with good precision.

To ensure a reasonably accurate treatment of hole scattering by acoustic phonons, we include in the present calculations (a) inelasticity, (b) spontaneous emission, and (c) the following truncated series expansion for the phonon occupation number according to Canali *et al.*[5]:

$$N_{\rm ph}(q) = \begin{cases} 1/x - 1/2 + x/12 - x^3/720, & x \leqslant 3.5, \\ 0, & x > 3.5. \end{cases} \tag{6}$$

Here, $x = \hbar sq/k_BT$, s is the velocity of sound, and q is the magnitude of the acoustic-phonon wave vector. The first

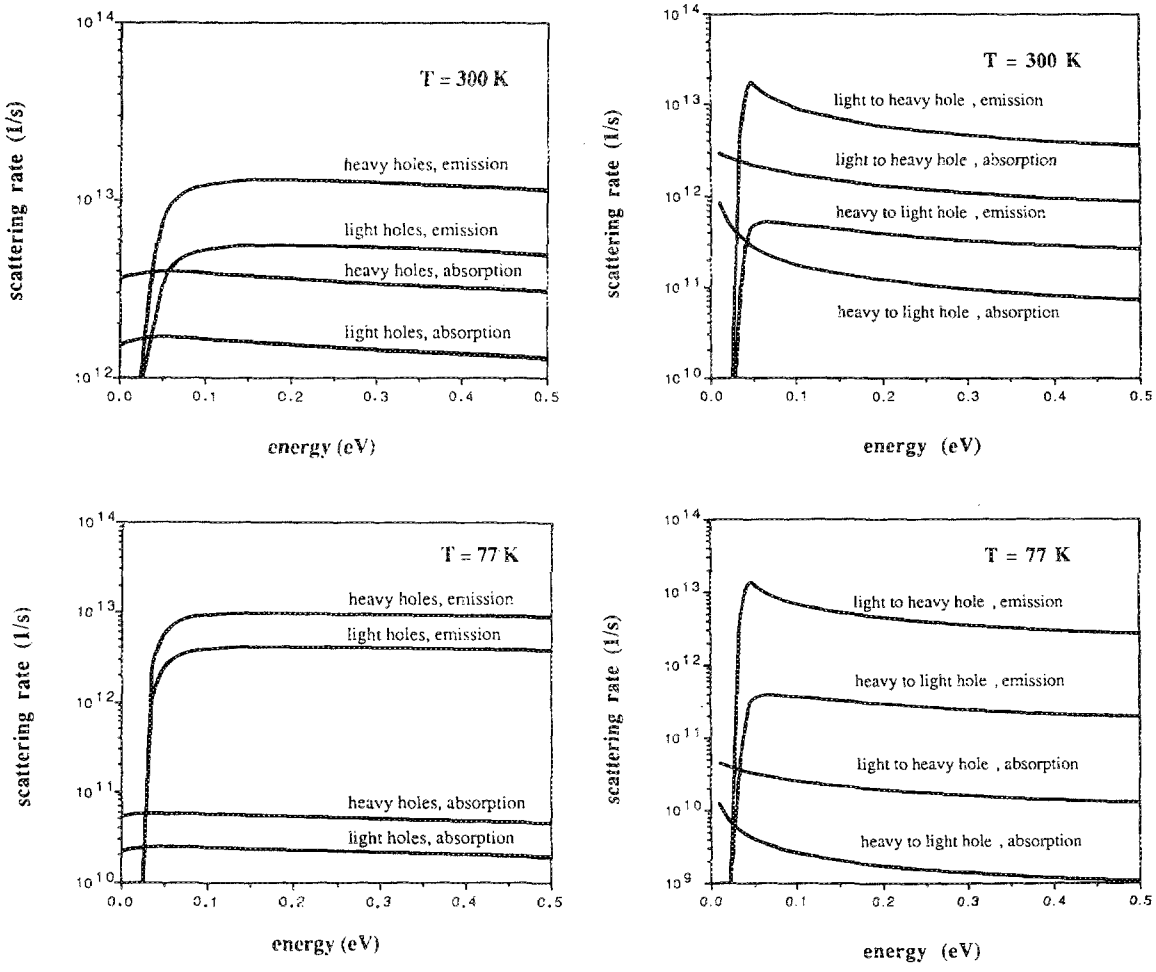

FIG. 3. Polar optical-phonon scattering rates for holes in GaAs for different temperatures.

term in $N_{\rm ph}(q)$ corresponds to the equipartition approximation. In Fig. 5, Eq. (6) is compared with the exact expression for the phonon occupation number $N_{\rm ph}(a) = [\exp(x) - 1]^{-1}$ and with the equipartition approximation. The relative importance of the different terms in Eq. (6) will be investigated later on in this report.

The *electron* acoustic deformation potential scattering rate in accordance with the above procedure was first calculated by Canali *et al.*[5] Later, this result was applied to holes in Refs. 3 and 4, but the overlap functions associated with warping in the valence bands were not properly taken into account. In addition, the interband scattering rate in Ref. 4 was set equal to the intraband rate of the final band. Although this equality is true in the usual elastic and equiparti-

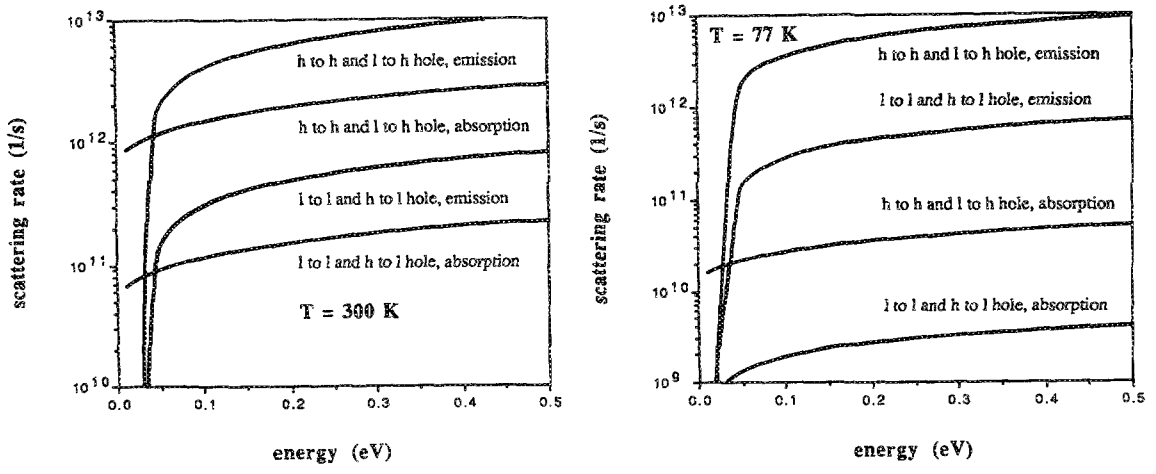

FIG. 4. Nonpolar optical-phonon scattering rates for holes in GaAs for different temperatures.

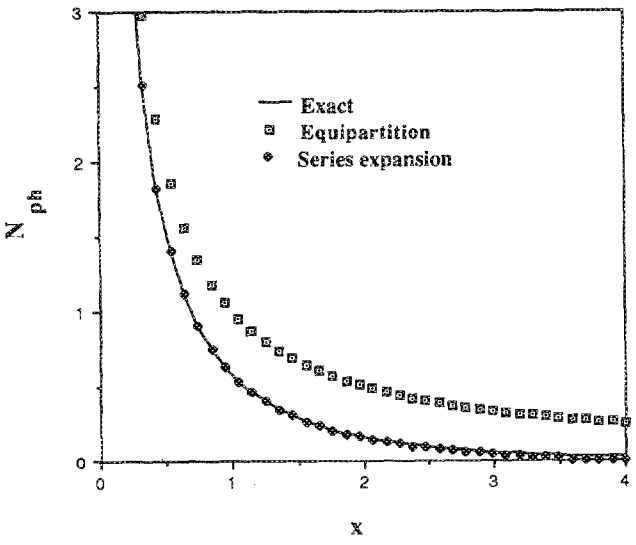

FIG. 5. The phonon occupation number. A comparison between the truncated series expansion, the equipartition approximation, and the exact expression.

tion approximations,[1] it does not strictly apply in the inelastic case. Accordingly, the integration limits used for x in Ref. 4 should be generalized to account properly for inelastic interband processes. Here, we follow the approach of Canali *et al.* and recalculate the hole acoustic scattering rates.

A. General expression for hole inelastic acoustic scattering rates

The hole acoustic deformation potential scattering rate P_{if}^{ac} can be expressed as

$$P_{if}^{ac}=\frac{E_1^2 k_B T}{2\rho(2\pi)^2\hbar s^2}\int d\mathbf{k}_f\, x\delta\left(\frac{\hbar^2 k_f^2}{2m_f}-\frac{\hbar^2 k_i^2}{2m_i}+E_t x\right)$$

$$\times\delta_{\mathbf{k}_f,\mathbf{k}_i\pm q}\begin{Bmatrix}N_{ph}(q)\\ N_{ph}(q)+1\end{Bmatrix} G(\theta_k) \qquad (7)$$

where E_1 is the acoustic deformation potential constant, and $\mathbf{k}_i$ and $\mathbf{k}_f$ are the initial- and final-state hole wave vectors, respectively. $E_t=-k_BT$ for absorption and $E_t=k_BT$ for emission of an acoustic phonon. Also, the factors $N_{ph}(q)$ and $N_{ph}(q)+1$ refer to absorption and emission of an acoustic phonon, respectively. $G(\theta_k)$ is the overlap function, which for inter- and intraband processes can be written as[1]

$$G^{inter}=3\sin^2(\theta_k)/4\,, \qquad (8a)$$

$$G^{intra}=[1+3\cos^2(\theta_k)]/4\,, \qquad (8b)$$

where θ_k is the angle between $\mathbf{k}_i$ and $\mathbf{k}_f$.

The conditioin $N_{ph}(q)=0$ for $x>3.5$ in Eq. (6) is most easily incorporated by performing the integration in Eq. (7) over $\mathbf{q}$, or equivalently, over x and the polar angle θ between $\mathbf{q}$ and the final-state wave vector $\mathbf{k}_f$. The scattering probability is assumed to be independent of the azimuthal angle φ. The relationship between the various variables is indicated in Fig. 6. The integration over θ is easily performed by means

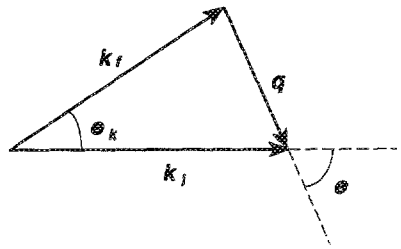

FIG. 6. Relationship between the various wave vectors involved in hole scattering by the emission of an acoustical phonon.

of the δ function expressing energy conservation. Conservation of energy and momentum leads to the following relationship between x and θ:

$$f(x)\equiv-(M-1)\hbar s k_i/2xE_t+E_t x/2\hbar s k_i+m_f s/\hbar k_i$$

$$=\cos(\theta). \qquad (9)$$

The lower limit (x_1) and the upper limit (x_2) of x are obtained from Eq. (9) using the condition $|\cos\theta|\leqslant 1$.[8]

B. Integration limits for emission

For emission, the limits of the integration variable x can be written as

$$x_1=\frac{2E_s^{1/2}}{k_BT}\{-C_+\pm[C_+^2+E(M-1)]^{1/2}\}\,, \qquad (10a)$$

$$x_2=\frac{2E_s^{1/2}}{k_BT}\{-C_-+[C_-^2+E(M-1)]^{1/2}\}\,, \qquad (10b)$$

where $E_S=\frac{1}{2}m_i s^2$, E is initial hole energy and $C_\pm=ME_s^{1/2}\pm E^{1/2}$. The upper and lower signs in Eq. (10a) correspond to $M>1$ and $M\leqslant 1$, respectively.

When $M\leqslant 1$, there is a threshold in E that must be exceeded in order for emission to be possible. By demanding that the argument of the square root in Eq. (10b) be positive and that x_1 and x_2 be positive, we find that

$$E\geqslant M^2E_s/[1-(1-M)^{1/2}]^2\,. \qquad (11)$$

For transitions from the heavy- to the light-hole band in GaAs, Eq. (11) requires that $E\geqslant 3.6E_s$. With $M=1$, i.e., for intraband processes, Eq. (11) reduces to the more familiar condition $E\geqslant E_s$.[8] At room temperature, k_BT is two orders of magnitude larger than E_s. Accordingly, this threshold is of practical importance only at low temperatures, typically below 10 K. When $M>1$, there is, of course, no threshold. In this case, a final state in the heavy-hole band can always be found such that both energy and momentum are conserved. The limits of integration for emission are illustrated in Fig. 7, which shows the function $f(x)$ of Eq. (9) for emission ($E_t=k_BT$) for two values of initial hole energy.

C. Integration limits for absorption

For absorption, the lower and upper limits of x become

$$x_1=\frac{2E_s^{1/2}}{k_BT}\{C_\mp\pm[C_\mp^2+E(M-1)]^{1/2}\}\,, \qquad (12a)$$

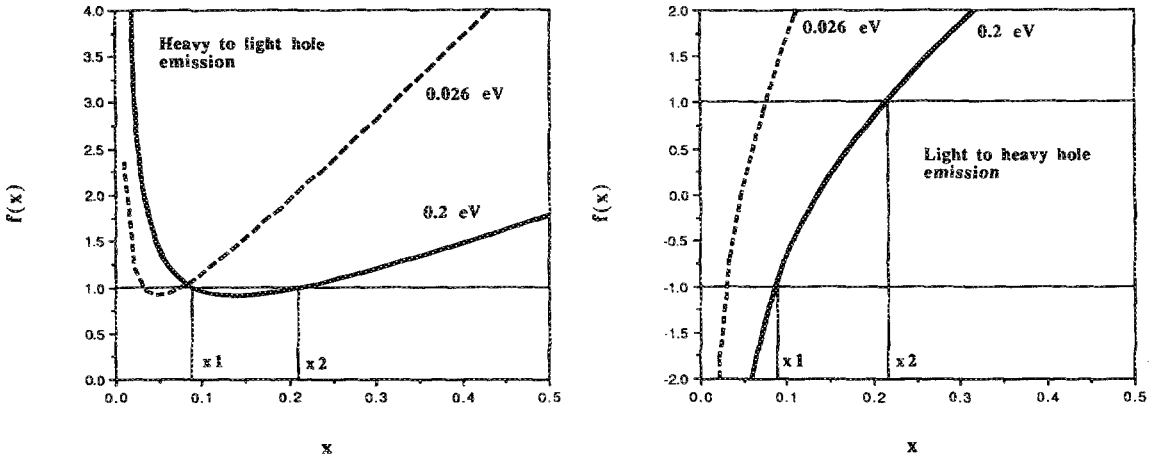

FIG. 7. The limits for the integration variable x in the case of interband hole scattering by the emission of an acoustic phonon, determined from the conditions of energy and momentum conservation. The limits are shown for two values of initial hole energy. $T = 300$ K.

$$x_2 = \frac{2E_s^{1/2}}{k_B T}\{C_+ + [C_+^2 + E(M-1)]^{1/2}\}, \quad (12b)$$

where again the upper and lower signs in Eq. (12a) correspond to $M > 1$ and $M \ll 1$, respectively.

When $M \ll 1$ and $E \ll M^2 E_s/[1 + (1-M)^{1/2}]^2$, the region between x_1 and x_2 given by Eqs. (12a) and (12b) is interrupted by a "forbidden" zone between

$$x_1' = \frac{2E_s^{1/2}}{k_B T}\{C_- - [C_-^2 + E(M-1)]^{1/2}\}, \quad (13a)$$

and

$$x_2' = \frac{2E_s^{1/2}}{k_B T}\{C_- + [C_-^2 + E(M-1)]^{1/2}\}. \quad (13b)$$

Fortunately, the latter region can be ignored in most cases, even at temperatures below 10 K. The limits of integration for absorption are illustrated in Fig. 8, which shows the function $f(x)$ of Eq. (9) for absorption ($E_t = -k_B T$) for two values of initial hole energy.

D. Resulting expressions for acoustic scattering rate

By performing the integration in Eq. (7), using the overlap functions in Eqs. (8a) and (8b) and the limits of integration defined in Eqs. (10a) and (10b), or Eqs. (12a) and (12b), the following expression can be derived for the acoustic deformation potential scattering rate in terms of initial hole energy:

$$P_{if}^{ac} = \frac{E_1^2 (k_B T)^3 m_i^{5/2}}{64\sqrt{2}\pi\rho\hbar^4 E_s^2} E^{-1/2}[B(E) + L(E)], \quad (14)$$

where

$$B(E) = \sum_{N=1}^{9} P_{BN}(E) B_N(x)\Big|_{x=x_{1l}}^{x=x_{1t}} + \sum_{N=2}^{6} P_{BN}^0(E) B_N(x)\Big|_{x=x_{2l}}^{x=x_{2t}} \quad (15)$$

and

$$B_N(x) = -\frac{1}{E_t}\sum_{n=1}^{N}\left(\frac{E}{E_t}\right)^{N-n}\frac{x^n}{n}. \quad (16)$$

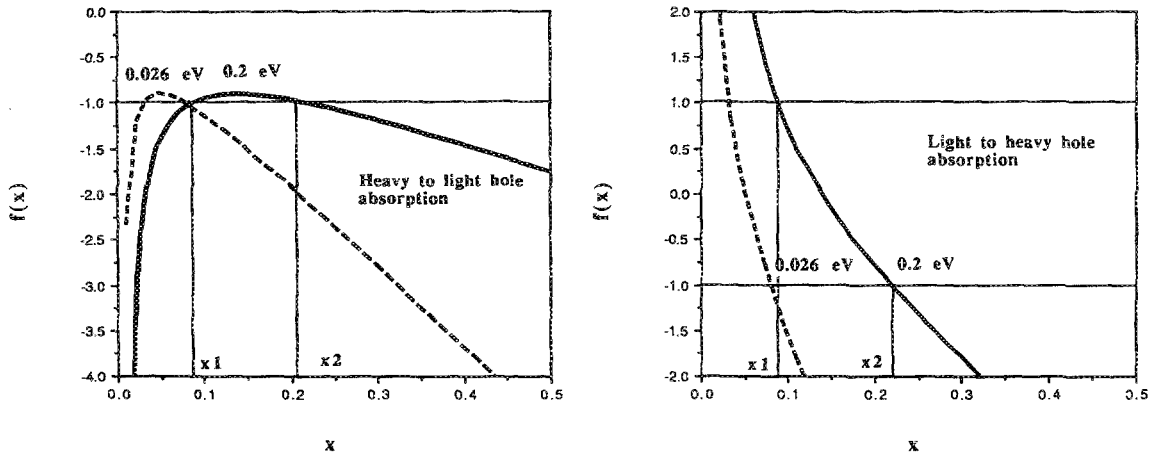

FIG. 8. The limits for the integration variable x in the case of interband hole scattering by the absorption of an acoustic phonon, determined from the conditions of energy and momentum conservation. The limits are shown for two values of initial hole energy. $T = 300$ K.

The functions $P_{BN}(E)$ and $P^0_{BN}(E)$ of Eq. (15) are listed in Table II for intraband scattering and in Table III for interband scattering. Note that the second sum in Eq. (15) is associated with spontaneous emission and should accordingly be omitted for absorption, i.e., $P^0_{BN}(E) = 0$ for absorption. The upper and lower limits x_U and x_L in the first sum in Eq. (15) (stimulated emission and absorption) reflect the fact that if x exceeds 3.5, $N_{\rm ph}(q)$ is set equal to zero [see Eq. (6)]. Thus $x_{U,L} = 3.5$ if $x_{2,1} > 3.5$ and $x_{U,L} = x_{2,1}$ if $x_{2,1} < 3.5$. For spontaneous emission, $N(q)$ does not enter, and x_1 and x_2 are always retained as limits.

The function $L(E)$ in Eq. (14) can be written as

$$L(E) = P_L(E)\ln\left(\frac{E - E_t x_U}{E - E_t x_L}\right) + P^0_L(E)\ln\left(\frac{E - E_t x_2}{E - E_t x_1}\right). \tag{17}$$

As before, the superscript 0 in the prefactor of the second term indicates a contribution from spontaneous emission, to be omitted in case of absorption. The function $P_L(E)$ and $P^0_L(E)$ are listed in Table IV.

The inelastic inter- and intraband acoustic deformation potential scattering rates for emission and absorption are shown in Fig. 9 for different temperatures. The parameters used are listed in Table I.

V. DISCUSSION

In the preceding sections we have presented the rates for the dominant scattering mechanism for holes in semiconductors. In particular, new results have been obtained for inelastic hole deformation potential scattering by acoustic phonons. The acoustic-phonon scattering results are therefore discussed separately in some detail in Sec. V A, whereafter a comparison of the different scattering mechanisms is presented in Sec. V B.

A. Acoustic-phonon scattering

Intuitively, one should expect the higher-order terms in the expansion of $N_{\rm ph}(q)$ in Eq. (6) to be important primarily for high-energy holes at low temperatures, where the equipartition approximation $[N_{\rm ph}(q) \approx 1/x]$ is most likely to fail. Here, we have kept track of the contribution from each term in $N_{\rm ph}(q)$ in order to see what effect the higher-order terms may have on the scattering rates under different circumstances.

The calculations show that, even at room temperature, the higher-order terms in $N_{\rm ph}(q)$ represent a non-negligible contribution to the scattering rates. Thus, for heavy-hole intraband scattering with absorption of acoustic phonons in GaAs, these terms cause a reduction of about 4% in the rate at a hole energy of $k_B T$, compared to the equipartition approximation. This figure increases steadily to 20% at 1 eV. For light holes, the difference was somewhat less owing to the smaller wave vectors involved for a given energy.

According to theory, the absorption rate exceeds the emission rate up to hole energies of about $2k_B T$ for a simple parabolic band.[8] For energies above $2k_B T$, the emission rate becomes the larger of the two. The different behavior for the two rates can be attributed to spontaneous emission and to inelastic effects. As a typical example, we consider the transition from the light- to heavy-hole band in GaAs at 300 K. At a hole energy of $k_B T$, the absorption rate exceeds the emission rate by about 9% when spontaneous emission is not included. This difference is, accordingly, caused by inelastic effects. Inclusion of spontaneous emission reduces the difference to 3%. At an energy of $4k_B T$, the stimulated emission rate is about 5% below the absorption rate, but inclusion of spontaneous emission now raises the total emission rate to 9% above the absorption rate. Thus, at energies above a few times $k_B T$, spontaneous emission is the dominant contributor to the difference in the absorption and emission rates. The higher scattering rate for emission should give rise to a cooling effect for the most energetic holes.[3–7]

From fig. 9, we also notice that the difference in the absorption and emission scattering rates is more pronounced for heavy holes than for light holes. The reason is that for a given energy, larger k vectors and, accordingly, larger values of x are involved in heavy-hole compared to light-hole scattering. Thus $N_{\rm ph}(q)$ is reduced, increasing the relative importance of spontaneous emission. The result is an enhanced separation of the emission and absorption curves for heavy holes.

For hole energies above $\hbar\omega_0$, emission of optical phon-

TABLE II. P_{BN} for *intraband processes* is in this table divided into a sum of four terms, i.e., $P_{BN}(E) = \Sigma_{I=1}^{4} P^{(I)}_{BN}(E)$, each originating in the corresponding term of the series expansion of $N(q)$. The term index $I = 1$–4 is counted from left to right in Eq. (6), with $I = 1$ corresponding to equipartition. Here, each $P^{(I)}_{BN}(E)$ is shown explicitly. $X(E) \equiv 1/E_s - 1/E$. For *spontaneous emission*: $P^0_{BN} = -2P^{(2)}_{BN}$.

N \ I	1	2	3	4
1	$4E$			
2	$-4E_t$	$-2E$		
3	$-3E_t^2X(E)/4$	$2E_t$	$E/3$	
4	$3E_t^3/8E_sE$	$3E_t^2X(E)/8$	$-E_t/3$	
5	$3E_t^4/64E_s^2E$	$-3E_t^3/16E_sE$	$-E_t^2X(E)/16$	$-E/180$
6		$-3E_t^4/128E_sE$	$E_t^3/32E_sE$	$E_t/180$
7			$E_t^4/256E_s^2E$	$E_t^2X(E)/960$
8				$-E_t^3/1920E_sE$
9				$-E_t^4/15\,360E_s^2E$

TABLE III. $P_{BN}(E)$ for *interband processes* is in this table divided into a sum of four terms, i.e., $P_{BN}(E) = \Sigma_{I=1}^{4} P_{BN}^{(I)}(E)$, each originating in the corresponding term of the series expansion of $N(q)$. The term index $I = 1$–4 is counted from left to right in Eq. (6), with $I = 1$ corresponding to equipartition. Here, each $P_{BN}^{(I)}(E)$ is shown explicitly. $Y(E) \equiv (M+1)/2E_s - M^2/E$. For *spontaneous emission*: $P_{BN}^{0} = -2P_{BN}^{(2)}$.

N \ I	1	2	3	4
1	$-3(1-M)^2E/4$			
2	$-3M(1-M)E_t/2$	$3(1-M)^2E/8$		
3	$3E_t^2Y(E)/4$	$3M(1-M)E_t/4$	$-(1-M)^2E/16$	
4	$-3ME_t^3/8E_sE$	$-3E_t^2Y(E)/8$	$-M(1-M)E_t/8$	
5	$-3E_t^4/64E_s^2E$	$3ME_t^3/16E_sE$	$E_t^2Y(E)/16$	$(1-M)^2E/960$
6		$3E_t^4/128E_s^2E$	$-ME_t^3/32E_sE$	$M(1-M)E_t/480$
7			$-E_t^4/256E_s^2E$	$-E_t^2Y(E)/960$
8				$ME_t^3/1920E_sE$
9				$E_t^4/15\,360E_s^2E$

ons becomes an alternative important loss mechanism since the optical emission rate rapidly exceeds the absorption rate. The acoustic-phonon scattering represents the sole loss mechanism for holes in the energy interval from about $2k_BT$ to $\hbar\omega_0 \approx 0.035$ eV (GaAs). For such an interval to exist, T must be less than 200 K, and the effect should be noticeable for intermediate field strengths[6] and long Monte Carlo simulation times. At higher field strengths, the holes are more rapidly heated up to energies in the range of $\hbar\omega_0$, where emission of optical phonons dominate the energy dissipation.

Eventually, for hole energies greater than 0.2 eV (GaAs, heavy-hole intraband scattering), the energy exchanged in acoustic scattering events approaches a value of about 10 meV.

Due to the complexity of the hole acoustic scattering rates, complications arise when trying to calculate final-state $\mathbf{k}$ vectors in Monte Carlo simulations. Canali *et al.*[5] proposed a procedure whereby a random number first is used to calculate x (or q) from the distribution function of x by means of the rejection technique. Then, the final state is determined by a geometrical construction which incorporates energy and momentum conservation. A disadvantage of this method is that the limit x_1 and x_2 vary with energy, whereas θ_k almost always retains the limits 0 and π. Tang[7] and Brennan[4] instead proposed a simplified technique based on the average of the energy exchanged in acoustic scattering processes. For $T > 10$ K, it is possible to calculate a preliminary $\mathbf{k}_f$, omitting inelasticity, from which approximate values for x (or q) can be found. Finally, a correction to $\mathbf{k}_f$, stemming from the small energy exchanged ($\hbar sq$), is made. For $T < 10$ K, the energy exchanged in a single event becomes comparable to k_BT for the most energetic carriers, and the approach by Canali *et al.* must be followed.

If the hole distribution becomes strongly shifted in the direction $\hat{\mathbf{e}}$ of the electric field, this direction will act as a reference for the polar angle θ_k in the overlap functions $G(\theta_k)$ (see Sec. IV A). Then, scattering into certain angles relative to $\hat{\mathbf{e}}$ will be favored, which makes the overlap functions important in determining $\mathbf{k}_f$ for individual events and, accordingly, in determining the shape of the hole distribution function. On the other hand, for a near-equilibrium Maxwellian distribution, the role of the overlap functions can be ignored in determining $\mathbf{k}_f$.

It is apparent from the results in Sec. IV D that the inclusion of both warping (through the overlap functions) and inelasticity makes the expressions for the scattering of holes by acoustic phonons very complex. The effect of warping *alone* would result simply in a multiplicative factor close to $\frac{1}{2}$ in the rates.[1,2] Our numerical calculations show that this continues to be true even when the series expansion for $N_{\text{ph}}(q)$ and inelastic effects are incorporated. It should be noted that a factor of exactly $\frac{1}{2}$ would result from averaging the overlap functions alone over all spatial angles (apparently, it is this factor which erroneously has become equal to 1 in the acoustic hole scattering rates of Ref. 4). In determining $\mathbf{k}_f$, however, it may still be important to include the overlap functions properly in the calculations in order to arrive at a correct distribution function in Monte Carlo simulations, as discussed above. In polar optical scattering, the proper inclusion of the overlap functions turns out to be crucial for avoiding a divergence in the scattering rate.[2]

The polynomials $B_N(x)$ that appear in the rates (see Sec. IV D) are nothing more than series expansions of $\ln(1 + E_t x/E)$, truncated after the Nth term and multiplied by $-(E_t/E)^N/E_t$. Accordingly, there is a close similarity between the term $B(E)$ and the logarithmic term $L(E)$ in

TABLE IV. $P_L(E)$ is for convenience written as a product of two terms, i.e., $P_L(E) = Q(E)P_{L1}(E)$. $P_{L1}(E)$ is divided into a sum of four terms, i.e., $P_{L1}(E) = \Sigma_{I=1}^{4} P_{L1}^{(I)}(E)$, each originating in the corresponding term of the series expansion of $N(q)$. The term index $I = 1$–4 is counted from left to right in Eq. (6), with $I = 1$ corresponding to equipartition. For *spontaneous emission*: $P_L^0 = -2P_L^{(2)}$. Here, each $P_{L1}^{(I)}(E)$ is shown explicitly for *intraband processes*. For *interband processes*, the only difference is a change in sign of all $P_{L1}^{(I)}(E)$ such that $P_{L,\text{inter}} = -P_{L,\text{intra}}$ and $P_{L,\text{inter}}^0 = -P_{L,\text{intra}}^0$. $Q(E) = -3E^2(1 - E/2E_s + E^2/16E_s^2)/4E_t^2$.

I	1	2	3	4
$P_{L1}^{(I)}(E)$	1	$-E/2E_t$	$E^2/12E_t^2$	$-E^4/720E_t^4$

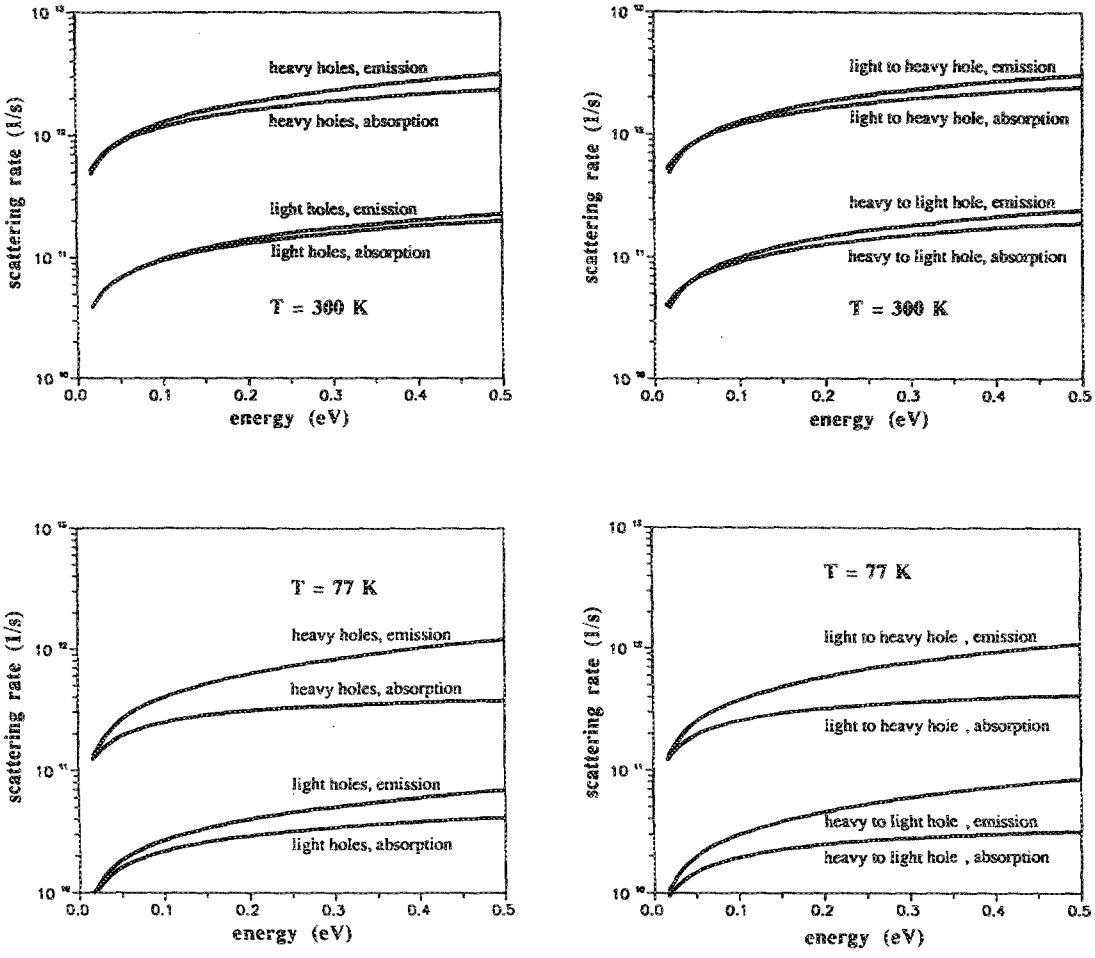

FIG. 9. Acoustic deformation potential scattering rates for holes in GaAs for different temperatures.

Eq. (14). This becomes apparent when calculating leading terms in E for the scattering rate, where a number of terms in the expansions of $B(E)$ and $L(E)$ cancel.

B. Comparison of hole scattering rates

All the various scattering mechanisms considered here contribute significantly to the overall transport properties of holes in cubic semiconductors, but not necessarily in proportion to their total scattering rates. Obviously, the amount of energy and momentum exchanged in individual events is very important. But even with little energy exchange and a relatively low scattering rate, a mechanism such as acoustic-phonon deformation potential scattering may still be an important channel for energy relaxation in a certain range of hole energies, as discussed previously. In the same range, other scattering rates, such as ionized impurity scattering, may be much larger. But ionized impurity scattering is elastic and therefore does not contribute to energy relaxation. Neither does it contribute much to momentum relaxation since small-angle scattering events dominate, particularly at higher energies.

A screened Coulomb potential according to Brooks and Herring[8] was used for calculating the ionized impurity scattering rate. This type of potential gives rise to a total intraband scattering rate that does not change much with impurity concentration, an artifact which is caused by a compensating tendency in the screening length. Thus a reduction in the impurity concentration gives rise to an increased screening length, but the fraction of low-angle scattering events increases such as to reduce the overall effect of impurity scattering on the hole transport.

At hole energies above the optical-phonon energy, the most important scattering mechanisms in pure GaAs appear to be the polar and nonpolar optical-phonon emission, with the former dominating over a wide range of energies. But, while the scattering rates for polar optical processes decrease with increasing hole energy, the rates for nonpolar emission increase steadily and become dominant in the high-energy end of the range investigated ($E < 0.5$ eV).

For hole energies below the optical-phonon energy, polar optical-phonon absorption is particularly important at room temperature. From the optical-phonon absorption rates, a rough estimate of the hole mobility in pure GaAs gives a value of about $\mu_h \simeq 500$ cm^2/(V s), which is in reasonable agreement with observations. At low energies, however, ionized impurity scattering is important in doped materials and will cause a further reduction in the mobility. The effect of acoustic phonon scattering has been discussed at length in Sec. V A. Here, we note that the acoustic scattering rates indeed are important at low temperatures (77 K and

lower) and at energies below the optical-phonon energy at all temperatures.

Our calculations show that interband scattering is dominant for light holes, but under normal conditions, the overall transport properties for holes are determined by heavy holes. However, the light- and heavy-hole band degeneracy at the center of the Brillouin zone may be lifted under stress, such that the light-hole band becomes the top valence band.[9] This effect is important for *p*-channel pseudomorphic InGaAs/GaAs heterostructure field-effect transistors (HFETs)[10,11] where it may enhance the low-field mobility. The obtained dependencies of scattering rates on energy clearly show that the hole velocity in high electric field should be enhanced by the band splitting under stress as well, because the interband scattering rates at high hole energy will be significantly dimished. (A typical band splitting in AlGaAs/InGaAs/GaAs pseudomorphic HFETs is estimated to be about 90 meV.[11]) This may have important implications for hole transport in short *p*-channel pseudomorphic HFETs because of a possibility of significant overshoot effects or even ballistic transport, especially for devices with variable threshold voltage where the electric field distribution in the channel is relatively uniform.

VI. SUMMARY

A number of modern semiconductor devices rely on hole transport. Consequently, dependable descriptions of hole transport properties in semiconductors are of great interest. On the microscopic scale, the physics involved in hole transport is reflected in the rates for the various scattering mechanisms. Unfortunately, previously published hole scattering rates are afflicted by numerous errors and misprints. We have therefore reviewed the rates for the dominant scattering mechanisms for holes in semiconductors, including ionized impurity scattering, polar and nonpolar optical scattering, and inelastic acoustic deformation potential scattering. In this paper, new and corrected results are presented, and the various rates are discussed and compared.

At hole energies above the optical-phonon energy, the most important scattering mechanisms in pure GaAs appear to be polar and nonpolar optical-phonon emission, with the former dominating over a wide range of energies. For hole energies below the optical-phonon energy, polar optical-phonon absorption is particularly important at room temperature. Acoustic deformation potential scattering and ionized impurity scattering (in doped materials) are also of significance, especially at low temperatures and in the low-energy range.

Some implications of the present results for Monte Carlo simulation of hole transport in semiconductors and semiconductor devices have also been discussed, including the importance of inelastic acoustic deformation potential scattering as a channel for energy relaxation at low fields. The problem associated with the calculation of the final-state wave vectors for this mechanism in Monte Carlo calculations has also been considered.

The effects of lifting the valence-band degeneracy at the Brillouin zone center is of considerable interest from a device point of view. Thus, in *p*-channel pseudomorphic HFETs, the associated band splitting may greatly enhance the hole transport efficiency by increasing the proportion of light holes over heavy holes while, at the same time, decreasing the interband scattering rate. Work is currently underway to further investigate such phenomena and to calculate the related two-dimensional hole scattering rates.

ACKNOWLEDGMENTS

This work was supported by the Royal Norwegian Council for Scientific and Industrial Research, the Minnesota Supercomputer Institute at the University of Minnesota, and the NATO Scientific Affairs Division.

[1] M. Costato and L. Reggiani, Phys. Status Solidi B **58**, 471 (1973).
[2] M. Costato and L. Reggiani, Phys. Status Solidi B **59**, 47 (1973).
[3] K. Brennan and K. Hess, Phys. Rev. B **29**, 5581 (1984).
[4] K. Brennan, Ph.D. thesis, University of Illinois, 1984.
[5] C. Canali, C. Jacoboni, F. Nava, G. Ottaviani, and A. Alberigi-Quaranta, Phys. Rev. B **12**, 2265 (1975).
[6] M. Artaki and K. Hess, Superlatt. Microstruct. **1**, 489 (1985).
[7] J. Y. Tang, Ph.D. thesis, University of Illinois, 1983.
[8] B. K. Ridley, *Quantum Processes in Semiconductors* (Clarendon, Oxford, 1988).
[9] G. L. Bir and G. E. Picus, in *Symmetry and Strain-Induced Effects in Semiconductors*, edited by D. Louvish (Wiley, New York, 1974).
[10] T. J. Drummond, T. E. Zipperian, I. J. Fritz, J. E. Schiber, and T. A. Plut, Appl. Phys. Lett. **49**, 461 (1986).
[11] P. P. Ruden, M. Shur, D. K. Arch, R. R. Daniels, D. E. Grider, and T. Nohava, IEEE Trans. Electron Devices **ED-36**, 2371 (1989).